MULTI-PASS INTERFEROMETER FOR QUANTITATIVE INVESTIGATION OF AXISYMMETRIC INHOMOGENEITIES IN RAREFIED GASES

I. V. Skokov and V. A. Emel'yanov

Inzhenerno-Fizicheskii Zhurnal, Vol. 11, No. 1, pp. 3–9, 1966

UDC 621.317.767

A multi-pass interferometer method has been used for visualization and determination of certain flow parameters of a rarefied gas in the slip flow regime over axisymmetric blunt models. An experimental determination has been made of the density distribution in the region of the forward stagnation point ahead of a sphere and of the shock wave profile ahead of a disk at M = 3.85 and Re = 75.

Because of the difficulty of direct solution of heat transfer problems in high-speed (~5 km/sec) flight at high altitude (~120 km), there is interest in improving and increasing the sensitivity of density diagnostic methods in a rarefied gas (Knudsen number ≥0.01). The density distribution around a model has a specific dependence on the temperature ratio T_W/T_0. Experimental determination of density gives information about shock wave structure, about the enthalpy of the rarefied gas stream, and about the heat loads acting on the model.

One of the effective ways of increasing the sensitivity of diagnostic methods for a rarefied gas is to use a multi-pass interferometer, employing multiple passes of the light wave through the inhomogeneity being studied [1, 2]. This method, in conjunction with photometric reading of the interferograms, allows registration of very small changes of refractive index in a nonuniform gas ($\Delta n \sim 10^{-6}$–10^{-7} in 1 cm length). However, the multi-pass interferometer has hitherto been used only for the study of plane flows, for example, in [2].

The present paper describes the results of an investigation of density distribution in a rarefied gas around an axisymmetric model. It should be mentioned that axisymmetric streams comprise a wide class of flows, investigation of which is a matter of great practical interest.

The experimental equipment consisted of a multi-pass interferometer (Fig. 1), the main element of which is a plane-parallel plate 4 provided with reflecting layers with R = 80%.

The collimating section consists of a light source 1 (water-cooled, high-pressure mercury lamp), an optical filter 2 (maximum transmission for 5770–5790 Å), and an objective 3 (focal length 300 mm).

The interferometer was arranged in such a way that the gas stream flowed between its mirrors. The interference pattern (uniformly illuminated interference field) was registered on the sensitive element 7 with the aid of objective 5 (focal length 300 mm), in the focal plane of which was mounted a diaphragm 6 of diameter 0.9 mm.

We used a photometric recording method, based on the dependence of the photographic density on the refractive index in the inhomogeneity under examination [2].

It is known [3] that the intensity distribution I in a multi-pass interference pattern has the form

$$I = I_m (1-R)^2 \Big/ \left[(1-R)^2 + 4R\sin^2\frac{\phi}{2}\right]. \quad (1)$$

It is assumed in (1) that there is no absorption in the medium, and that collimated monochromatic light falls on the interferometer plates at an angle φ close to $\pi/2$. In that case the expression for the phase difference may be written as

$$\phi = \frac{4\pi nl}{\lambda} + \delta + \delta'. \quad (2)$$

If the refractive index of a gaseous inhomogeneity n differs from the value n_0 in the undisturbed medium, we may write

$$\Delta\phi = \frac{4\pi}{\lambda}\int_{-x}^{x}(n-n_0)\,dx, \quad (3)$$

where dx is expressed in terms of the variable radial coordinate of the inhomogeneity in the form

$$dx = 2rdr/(r^2-y^2)^{1/2}. \quad (4)$$

At the same time, it is known from [2] and [3] that

$$\Delta\phi = \frac{2.3\,(s_y-s_0)}{\gamma}\,\frac{(1-R)}{\sqrt{R}}\,\frac{[1+2.3\,(s_m-s_0)/\gamma]}{2\,[2.3\,(s_m-s_0)/\gamma]^{1/2}}. \quad (5)$$

Then, after a number of transformations of (3)–(5) we obtain

$$\frac{\lambda}{k}(s_y-s_0) = \xi\int_{y}^{r_0}\frac{(\rho-\rho_0)\,rdr}{(r^2-y^2)^{1/2}}, \quad (6)$$

where

$$\xi = \frac{16\pi\gamma}{2.3}\left[2.3\,\frac{s_m-s_0}{\gamma}\,R\right]^{1/2}\Big/ \Big/\left[1+2.3\,\frac{s_m-s_0}{\gamma}\right](1-R). \quad (7)$$

The density difference between some point y in the inhomogeneity and the value ρ_0 in the undisturbed region is

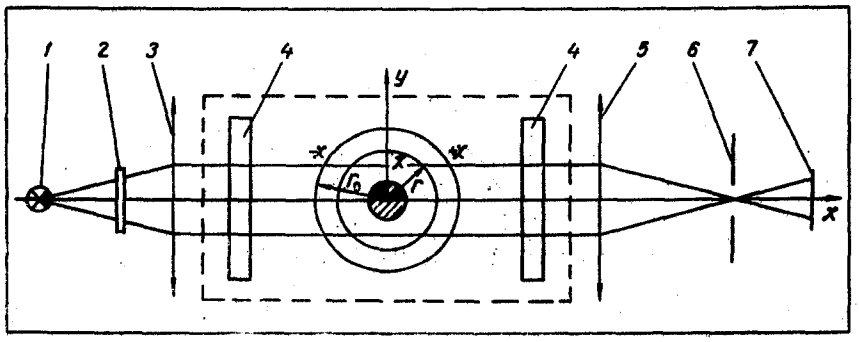

Fig. 1. Experimental set-up.

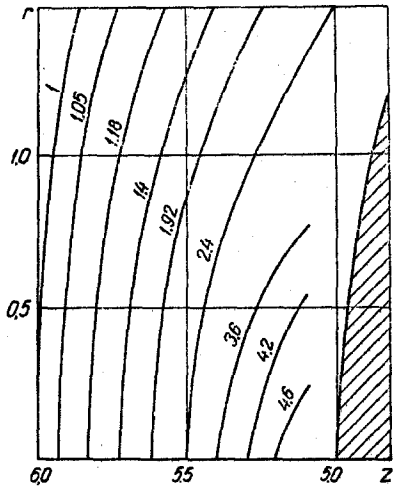

Fig. 2. Density field around a sphere washed by a stream of rarefied gas (the numbers on the curves give the ratio ρ/ρ_∞).

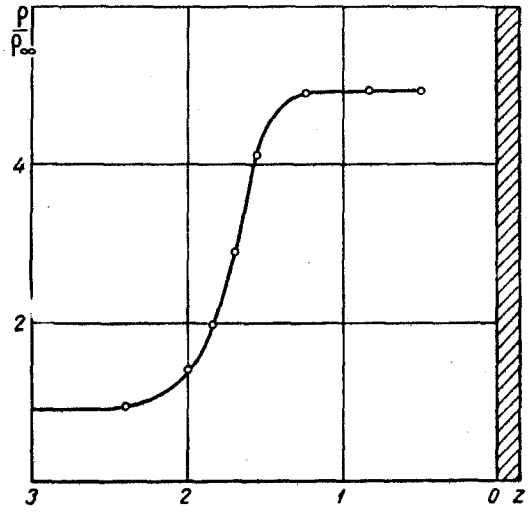

Fig. 3. Shock wave profile ahead of a disk (Re = 75, M_∞ = 3.85, $T_0 \cong 300°$ C).

$$\rho_y - \rho_0 = -\frac{\lambda}{\pi k \xi \bar{y}} \frac{d}{d\bar{y}} \int_{\bar{r}_i}^{1} \frac{(s - s_0)\bar{r}d\bar{r}}{(\bar{r}^2 - \bar{r}_i^2)^{1/2}}, \quad (8)$$

where $\bar{r}_i = y/r_0$, $\bar{r} = r/r_0$.
The function

$$\psi(\bar{y}) = \int_{\bar{r}_i}^{1} \frac{(s - s_0)\bar{r}d\bar{r}}{(\bar{r}^2 - \bar{r}_i^2)^{1/2}} \quad (9)$$

is a smoother function than $s_y - s_0$. Therefore the differentiation with respect to y in (8) is carried out, after an approximate evaluation of the integral (9), to increase the accuracy of the method. The cross section of an axisymmetric inhomogeneity is divided into a finite number N of annular zones, in each of which the film density difference $s(\bar{r}) - s_0$ is approximated by a second-degree polynomial. From the experimentally obtained values of $s - s_0$ at the boundary points and at the central point of a zone,

$$s(\bar{r}) - s_0 \simeq \sum_{k=1}^{3} l_j^{(k)} s(\bar{r}_k), \quad (10)$$

where

$$l_j^{(k)} = F_j(\bar{r})/(\bar{r} - \bar{r}_{j+k-1}) F_j'(\bar{r}_{j+k-1}), \quad (11)$$

$$F_j(\bar{r}) = (\bar{r} - \bar{r}_j)(\bar{r} - \bar{r}_{j+1})(\bar{r} - \bar{r}_{j+2}). \quad (12)$$

Substituting (11) and (12) into the expression for ψ, we obtain, after integration,

$$\psi(\bar{r}_i) = \sum_{j=\frac{1}{2}}^{N-1} \sum_{k=1}^{3} \alpha_{j,2j}^{k} s(\bar{r}_{2j+k-1}). \quad (13)$$

Here

$$\alpha_{j,2j}^{k} = \frac{1}{\pi F'(\bar{r}_{2j+k-1})} \int_{\bar{r}_{2j}}^{\bar{r}_{2j+2}} \frac{F(\bar{r})\bar{r}d\bar{r}}{(\bar{r} - \bar{r}_{2j+k-1})(\bar{r}^2 - \bar{r}_i^2)^{1/2}}. \quad (14)$$

For differentiation of $\psi(\bar{r}_i)$ with respect to $\bar{r}_i$, we approximate $\psi(\bar{r})$ in the form

$$\psi(\bar{r}) = \sum_{k=1}^{3} \frac{F(r)}{(\bar{r} - \bar{r}_{i+k-2}) F'(\bar{r}_{i+k+2}) \psi(\bar{r}_{i+k-2})}. \quad (15)$$

Then

$$\frac{d\psi(\bar{r}_i)}{d\bar{r}_i} = N[\psi(\bar{r}_{i+1}) - \psi(\bar{r}_{i-1})], \quad (16)$$

and after a series of transformations (8) is reduced to the form

$$\rho(\bar{r}_i) - \rho_0 = \frac{\lambda}{k\xi} \left\{ \sum_{j=i-1}^{2N-1} \beta_{ji} [s(\bar{r}_j) - s_0] \right\}. \quad (17)$$

In a rarefied gas flow with $M_\infty > 1$ over blunt bodies, no concentrated density discontinuity is formed around the model, as occurs in continuum gasdynamics. The density variation proceeds more smoothly, and the experimental function $s(r) - s_0$ is smoother in comparison with the distribution of interference fringe shifts in the case when a density discontinuity is formed in a continuum.

To reduce the amount of input data and the time required to calculate density (without impairing the accuracy of approximation to the function $s(\bar{r}) - s_0$), it is expedient to divide the section of the inhomogeneity into a small number of zones. However, it is then necessary to calculate $\rho(\bar{r}) - \rho_0$ at more points, not only at the nodes, but also at intermediate points of the zone.

For solving such problems we have calculated and tabulated coefficients $\beta_{j,i}$ which permit determination of the quantity $\rho(r_i) - \rho_0$ at the system of nodal points with subdivision into 25 zones: $\{\bar{r}_i\} = 0.04, \ldots, 0.90$ by 0.02 from values of the photographic density difference at nodal points r_j, corresponding to division into 5 zones: $r_j = 0.02, 0.1, \ldots, 0.9$ by 0.1 (see table).

In the table the coefficients $\beta_{j,i}$ (five-place numbers) are arranged by columns. Above each coefficient column is given the value of the coordinate $\bar{r}_i$, at which the desired quantity $\rho(\bar{r}_i) - \rho_0$ is calculated, and to the left of the coefficient columns there are values of the coordinate $\bar{r}_j$ at which the experimental functions $s(\bar{r}_j) - s_0$ are determined. The coefficients $\beta_{j,i}$ are multiplied in pairs by the corresponding quantities $s(\bar{r}_j) - s_0$, and give the value of $\rho - \rho_0$ at point $\bar{r}_i$, as a result of summation, according to (17). For example, to calculate $\rho - \rho_0$ at the point $\bar{r}_i = 0.04$, the coefficients 6.0735, −3.5850, ..., −0.0163 (first column of coefficients $\beta_{j,i}$ of the table) are multiplied in pairs by the values $s(\bar{r}_j) - s_0$ determined at the points $r_j = 0.02, 0.1, \ldots, 0.98$.

It may be seen from the table that the points $\bar{r}_j$ are nodes (extreme and central) of the zones corresponding to N = 5, while $\bar{r}_i$ are nodes of zones corresponding to N = 25.

In the present paper these coefficients are used to determine the density at points near the center of the section of the inhomogeneity. It then becomes possible to determine $\rho(\bar{r}_i)$ at small $\bar{r}_i (\bar{r} = 0.04)$, which allows the density variation to be traced along the axis of the stream, detailed investigation of the shock wave structure, and evaluation of the shock stand-off distance from the model.

The method described was used for the quantitative investigation of a supersonic rarefied gas flow over blunt bodies.

Figure 2 shows the density field around a sphere 10 mm in diameter in the region of the forward stagnation point. The abscissa is distance from the model along the stagnation streamline, and the ordinate—distance from the axis of the stream. The experimental curves are lines of equal density ahead of the sphere. This picture was obtained with the following oncoming flow parameters: $M_\infty = 3.85$, Re = 75 (the Reynolds number was calculated from stream parameters behind the shock and the sphere radius), $T_0 \cong$ ≅ 300° C.

Table

Coefficients β for Determining $\rho(\bar{r}_i) - \rho_0$ with N = 5

$\bar{r}_j$	Coefficients					
	$\bar{r}_i$=0.04	$\bar{r}_i$=0.06	$\bar{r}_i$=0.08	$\bar{r}_i$=0.10	$\bar{r}_i$=0.12	$\bar{r}_i$=0.14
0.02	6.0735	3.6842	1.8334	0.4322		
0.10	—3.5850	—0.5356	1.9944	3.8937	3.6928	2.6467
0.20	—1.3725	—2.0082	—2.8042	—3.4091	—2.4175	—0.8628
0.30	—0.1575	—0.1770	—0.0424	—0.0770	—0.2544	—0.7398
0.40	—0.2815	—0.2807	—0 2962	—0.3008	—0.3243	—0.3363
0.50	—0.0805	—0.0853	—0.0823	—0.0880	—0.0853	—0.0921
0.60	—0.1209	—0.1194	—0.1235	—0.1228	—0.1281	—0.1284
0.70	—0.0424	—0.0445	—0.0427	—0.0453	—0.0439	—0.0466
0.80	—0.0656	—0.0647	—0.0662	—0.0657	—0.0676	—0.0672
0.90	—0.0316	—0.0318	—0.0319	—0.0323	—0.0323	—0.0328
0.98	—0.0163	—0.0169	—0.0164	—0.0172	—0.0166	—0.0175
$\bar{r}_j$	$\bar{r}_i$=0.16	$\bar{r}_i$=0.18	$\bar{r}_i$=0.20	$\bar{r}_i$=0.22	$\bar{r}_i$=0.24	$\bar{r}_i$=0.26
0.10	1.7965	1.1001	0.6849	0.1080	—0.1998	—0.4005
0.20	0.3453	1.2887	1.3050	2.4166	2.5886	2.5521
0.30	—1.0555	—1.2635	—0.5888	—1.2636	—1.0031	—0.6438
0.40	—0.3724	—0.3968	—0.6666	—0.5062	—0.6250	—0.7238
0.50	—0.0895	—0.0975	—0.0767	—0.1028	—0.0938	—0.1043
0.60	—0.1349	—0.1363	—0.1536	—0.1475	—0.1583	—0.1632
0.70	—0.0454	—0.0484	—0.0489	—0.0508	—0.0499	—0.0539
0.80	—0.0696	—0.0695	—0.0761	—0.0724	—0.0755	—0.0762
0.90	—0.0330	—0.0336	—0.0341	—0.0346	—0.0350	—0.0359
0.98	—0.0170	—0.0179	—0.0143	—0.0184	—0.0179	—0.0190
$\bar{r}_j$	$\bar{r}_i$=0.28	$\bar{r}_i$=0.30	$\bar{r}_i$=0.32	$\bar{r}_i$=0.34	$\bar{r}_i$=0.36	$\bar{r}_i$=0.38
0.10	—0.3812					
0.20	1.8804	0.6226				
0.30	0.4063	1.0330	2.3287	1.7329	1.2132	0.7624
0.40	—1.1671	—0.4797	—1.4272	—0.4900	0.2920	0.9405
0.50	—0.3871	—0.5302	—0.1573	—0.4735	—0.6979	—0.8589
0.60	—0.1775	—0.0644	—0.2054	—0.2186	—0.2478	—0.2701
0.70	—0.0532	—0.1273	—0.0572	—0.0628	—0.0621	—0.0685
0.80	—0.0799	—0.0413	—0.8856	—0.0874	—0.0929	—0.0954
0.90	—0.0364	—0.0649	—0.0381	—0.0394	—0.0402	—0.0418
0.98	—0.0186	—0.0062	—0.0194	—0.0208	—0.0204	—0.0219
$\bar{r}_j$	$\bar{r}_i$=0.40	$\bar{r}_i$=0.42	$\bar{r}_i$=0.44	$\bar{r}_i$=0.46	$\bar{r}_i$=0.48	$\bar{r}_i$=0.50
0.30	0.5649	0.0761	—0.1499	—0.3027	—0.2926	
0.40	0.8820	1.7806	1.9334	1.9310	1.4442	0.5186
0.50	—0.4135	—0.8958	—0.7206	—0.4628	0.3268	0.7825
0.60	—0.4509	—0.3593	—0.4523	—0.5334	—0.8766	—0.3683
0.70	—0.0559	—0.0745	—0.0690	—0.0776	—0.0289	—0.3980
0.80	—0.1103	—0.1060	—0.1149	—0.1203	—0.1320	—0.0498
0.90	—0.0433	—0.0447	—0.0459	—0.0482	—0.0498	—0.0983
0.98	—0.0180	—0.0233	—0.0231	—0.0251	—0.0250	—0.0077

Table (cont'd)

$\bar{r}_j$	Coefficients					
	$\bar{r}_i$=0.52	$\bar{r}_i$=0.54	$\bar{r}_i$=0.56	$\bar{r}_i$=0.58	$\bar{r}_i$=0.60	$\bar{r}_i$=0.62
0.50	1.8394	1.3820	0.9761	0.6182	0.4815	0.0620
0.60	—1.1039	—0.3717	0.2510	0.7762	0.7106	1.4752
0.70	—0.1212	—0.3731	—0.5561	—0.6905	—0.3351	—0.7306
0.80	—0.1562	—0.1683	—0.1926	—0.2126	—0.3598	—0.2881
0.90	—0.0544	—0.0580	—0.0602	—0.0644	—0.0565	—0.0712
0.98	—0.0273	—0.0306	—0.0303	—0.0334	—0.0295	—0.0380
$\bar{r}_j$	$\bar{r}_i$=0.64	$\bar{r}_i$=0.66	$\bar{r}_i$=0.68	$\bar{r}_i$=0.70	$\bar{r}_i$=0.72	$\bar{r}_i$=0.74
0.50	—0.1251	—0.2532	—0.2463			
0.60	1.6100	1.6161	1.2162	0.4510		
0.70	—0.5904	—0.3789	0.2807	0.6554	1.5680	1.1834
0.80	—0.3659	—0.4360	—0.7246	—0.3094	—0.9250	—0.3035
0.90	—0.0701	—0.0761	—0.0396	—0.3306	—0.1213	—0.3355
0.98	—0.0391	—0.0441	—0.0461	0.0052	—0.0561	—0.0652
$\bar{r}_j$	$\bar{r}_i$=0.76	$\bar{r}_i$=0.78	$\bar{r}_i$=0.80	$\bar{r}_i$=0.82	$\bar{r}_i$=0.84	$\bar{r}_i$=0.86
0.70	0.8392	0.5335	0.4255	0.0536	—0.1095	—0.2221
0.80	0.2227	0.6849	0.6114	1.3009	1.4300	1.4410
0.90	—0.4972	—0.6173	—0.3327	—0.6673	—0.5687	—0.3857
0.98	—0.0714	—0.0852	—0.1281	—0.1208	—0.1488	—0.1946
$\bar{r}_j$	$\bar{r}_i$=0.88	$\bar{r}_i$=0.90				
0.70	—0.2168	—0.3782				
0.80	1.1322	1.0716				
0.90	0.0923	0.5628				
0.98	—0.3106	—0.5949				

Analysis of the density distribution shows that with the above stream parameters a zone of relatively constant density is observed behind the shock. Its value behind the shock agrees, to within the experimental accuracy, with that calculated from the Hugoniot relation. The density increase proceeds more slowly at the beginning of the shock layer than at its end.

Figure 3 shows the experimental shock profile for a flow at $M_\infty = 3.85$, $Re = 75$, $T^0 \cong 300°$ C over a disk 10 mm in diameter. As in the case of flow over a sphere, the shock wave is broadened, and a constant density section occurs behind the shock for which the Hugoniot relation holds. For the disk, however, a greater shock layer stand-off distance is observed, and a more extensive constant density region behind the shock.

The data obtained are in good agreement with the results of recent investigations of a rarefied gas by a method based on electron beam scattering [7]. This speaks for the effectiveness of using the multi-pass interferometer for diagnosis of a supersonic gas flow at low density, which provides sufficiently high measurement accuracy when the above calculation technique is used.

NOTATION:

T_0 is the stagnation temperature; T_ω is the wall temperature; R is the reflectivity of interferometer mirrors; ϕ is the phase difference of neighboring interferometer rays; I is the light intensity in interferogram; λ is the wavelength of light; k is the Gladstone-Dale constant; δ, δ' are the phase discontinuities at mirror surfaces; l is the geometric length of ray path in inhomogeneity; γ is the contrast of photographic material; s is the photographic density; r_0 is the radius of axisymmetric inhomogeneity; ρ is the density; M is the Mach number. The subscript 0 refers to the undisturbed flow, y to the point under study in the disturbed region, and m to points located at maximum intensity in the interferogram.

REFERENCES

1. F. A. Korolev, G. I. Kromskoi, and I. V. Skokov, Izv. VUZ. Fizika, no. 5, 1963.

2. F. A. Korolev, A. I. Akimov, G. I. Kromskoi, and I. V. Skokov, Pribory i tekhnika eksperimenta, no. 4, 1965.

3. F. A. Korolev, High-Resolution Spectroscopy [in Russian], GITTL, 1953.

4. I. V. Skokov, Vestnik MGU, Fizika, no. 2, 1962.

5. V. A. Emel'yanov and G. P. Zhavrid, IFZh, no. 5, 1962.

6. V. A. Emel'yanov, IFZh, no. 6, 1963.

7. A. V. Ivanov, DAN SSSR, **161**, 315, 1965.

19 January 1966